



Direct measurements of ${}^2\text{H}(\alpha, \gamma){}^6\text{Li}$ cross section at Big Bang energies and the primordial lithium problem

P. Colombetti^{1,2} and G. Gervino^{1,2}

¹ Dipartimento di Fisica, Università di Torino, e-mail: paolo.colombetti@unito.it

² INFN Sezione di Torino

Abstract. The correct prediction of the abundances of the light nuclides produced during of Big Bang Nucleosynthesis (BBN) is one of the main topics of modern cosmology. In order to precisely determine BBN ${}^6\text{Li}$ production the cross-section of the nuclear reaction ${}^2\text{H}(\alpha, \gamma){}^6\text{Li}$ must be directly measured within the astrophysical energy range of 30-400 keV. This measurement requires ultra low gamma-ray background, as obtained at LUNA, the deep underground accelerator laboratory installed in the INFN Gran Sasso National Laboratory (LNGS), Italy. On the basis of the new experimental data, the ${}^2\text{H}(\alpha, \gamma){}^6\text{Li}$ thermonuclear reaction rate has been derived. Our rate is even lower than previously reported, thus increasing the discrepancy between predicted Big Bang ${}^6\text{Li}$ abundance and the amount of primordial ${}^6\text{Li}$ inferred from observations. The primordial ${}^6\text{Li}/{}^7\text{Li}$ isotopic abundance ratio has been consequently determined to be $(1.5 \pm 0.3) \times 10^{-5}$ within standard BBN theory. The much higher ${}^6\text{Li}/{}^7\text{Li}$ values reported for halo stars will likely require a non-standard physics explanation, as discussed in the literature.

Key words. Nucl. Astrophysics, Big Bang Nucleosynthesis, ${}^6\text{Li}$ abundance, Underground

1. Introduction

The light isotopes such as ${}^2\text{H}$, ${}^3\text{He}$, ${}^4\text{He}$, ${}^6\text{Li}$ and ${}^7\text{Li}$ were mostly produced in the first few minutes after the Big Bang, during a process known as standard big bang nucleosynthesis (BBN) and BBN could be used to probe the cosmological models and their parameters. The BBN nuclear reaction rates are proportional to initial light nuclei densities, which are themselves proportional to the total baryon density. The observed ${}^2\text{H}$ and ${}^4\text{He}$ abundances are in good agreement with model predictions, confirming the overall validity of BBN theory (Hinshaw et al. 2013). By contrast, the

amount of ${}^7\text{Li}$ expected by BBN is higher than that observed in the metal-poor halo stars (the so-called “lithium problem” in Fields 2011). BBN ${}^7\text{Li}$ predictions are now a factor between 2 and 4 higher than observations (Spite & Spite 1982) and up to now a solution to the lithium problem has not been found (${}^7\text{Li}$ isotopic abundance on Earth: 92.41%) even though some possible stellar solutions have been suggested (Korn et al. 2006). Even more complicated is the case of ${}^6\text{Li}$ (isotopic abundance on Earth: 7.59%), where the amount of ${}^6\text{Li}$ calculated by the BBN is about three orders of magnitude lower than the observation values in metal-poor stars (the so-called

“second lithium problem”). Lithium measurements of many metal-poor stars give the isotopic ratio ${}^6\text{Li}/{}^7\text{Li}$ around $5 \cdot 10^{-2}$ where BBN predicts a value of ${}^6\text{Li}/{}^7\text{Li} \sim 2.3_{-2}^{+3} 10^{-5}$ (Pérez et al. 2009). Even though many of the claimed ${}^6\text{Li}$ measurements could have been affected by large uncertainty (Pérez et al. 2009; Steffen et al. 2010) in the past, nowadays more and more metal-poor stars have been observed improving the knowledge about ${}^6\text{Li}$ isotopic (Steffen et al. 2012): this value is still much higher than the predicted ${}^6\text{Li}$ yield from standard Big Bang nucleosynthesis (Serpico et al. 2004). Discrepancy between primordial Li abundance prediction and isotopic lithium ratio with experimental evidences could reflect unknown post-primordial processes or physics beyond the standard model (Hinshaw et al. 2013). However, before non-standard scenarios can be put forward, it is necessary to better constrain the nuclear physics inputs. BBN ${}^6\text{Li}$ abundance is dominated by two nuclear reactions: the ${}^6\text{Li}(p, \alpha){}^3\text{He}$ reaction that destroys ${}^6\text{Li}$ and the ${}^2\text{H}(\alpha, \gamma){}^6\text{Li}$ that produces it, both reactions are included in the research program of nuclear astrophysics LUNA at Gran Sasso Underground National Laboratories. ${}^2\text{H}(\alpha, \gamma){}^6\text{Li}$ reaction rate before LUNA data was affected by large uncertainties due to the scarcity of experimental data at BBN energies, therefore its cross-section to cover the BBN energy window (30–400 keV) has been measured by high sensitive γ spectrometry technique in order to put the discussion on this fundamental nuclear reaction in the framework of solid experimental ground. LUNA measured the cross section at the center-of-mass energy $E = 133, 120, 93$ and 80 keV and the experimental results are here presented and discussed.

2. The nuclear physics of primordial ${}^6\text{Li}$

${}^6\text{Li}$ is mainly produced during the BBN and, in recent time, by cosmic ray spallation (Reeves et al. 1970). Its primordial abundance is inferred from observations of the atmospheres of metal-poor stars in the galactic halo (either main sequence dwarfs or subgiants near the

turn-off point), therefore the primordial abundance is obtained by extrapolating the abundance at zero metallicity. The strength of the lithium absorption line ($\lambda = 670.7$ nm) provides the lithium abundance. As the absorption line of ${}^6\text{Li}$ is slightly shifted towards a higher wavelength compared to ${}^7\text{Li}$, the abundance of ${}^6\text{Li}$ isotope can be obtained through the shape analysis of the lithium absorption line. This shape is also affected by uncertainties related to the convective motions of the stellar atmosphere. According to Steffen et al. (2012) and Lind et al. (2013), it has been shown that using three-dimensional model for stellar atmosphere without the assumption of Local Thermodynamic Equilibrium (3D-NLTE), many of the ${}^6\text{Li}$ values could be heavily model dependent and may become non-significant, but the situation is still unclear. The 3D-NLTE analysis of star HD 84937 provides contradictory results according to different authors (Steffen et al. 2012; Lind et al. 2013), in other cases, such as star G020-024 for instance, we have a good agreement between one dimensional (Asplund et al. 2006) and three dimensional models (Steffen et al. 2012), respectively. The ${}^2\text{H}(\alpha, \gamma){}^6\text{Li}$ reaction is the dominant nuclear reaction for ${}^6\text{Li}$ production in standard BBN. In the low-energy domain, the cross section $\sigma(E)$ is usually parameterized throughout the astrophysical S-factor $S(E)$ defined by

$$S(E) = E \sigma(E) \exp(2\pi\eta(E)),$$

with E the center-of-mass energy, and $2\pi\eta(E)$ the Sommerfeld parameter taking into account the energy dependence probability of tunneling through the Coulomb barrier. The ${}^2\text{H}(\alpha, \gamma){}^6\text{Li}$ cross section at energies less than 1 MeV is dominated by radiative $E2$ capture from d waves in the scattering state into the ground state of ${}^6\text{Li}$ through the $3+$ resonance at $E_R = 711$ keV. At energies lower than 300 keV in the center-of-mass system, due to the different angular momentum barriers for p and d waves, the $E1$ contribution is expected to be comparable to $E2$ (Hammache et al. 2010; Nollett 2001). This reaction has been studied before LUNA by in-beam γ -spectrometry around the $E = 0.711$ MeV resonance (Mohr et al. 1994). At even higher

energies, there are data by in-beam detection of the ${}^6\text{Li}$ reaction products (Robertson et al. 1981). In both cases (Mohr et al. 1994; Robertson et al. 1981), an α -beam strikes on a deuterium gas target. A third kind of experiment at very low energy, using a deuterated polyethylene target, has produced an upper limit (Cecil et al. 1996). Two independent attempts to determine the ${}^2\text{H}(\alpha, \gamma){}^6\text{Li}$ cross section have been made using the Coulomb dissociation technique (Hammache et al. 2010; Kiener et al. 1991), which is especially sensitive, but also affected by heavy background from non-Coulomb, i.e. nuclear breakup (Baur & Rebel 1996). In conclusion, the ${}^6\text{Li}$ abundance predicted by the BBN theory is affected by large uncertainties because of the lack of data for the ${}^2\text{H}(\alpha, \gamma){}^6\text{Li}$ reaction. In this context, the LUNA measurement discussed in this paper represents a significant step forward, providing the first direct measurement of this reaction well inside the BBN energy region.

3. Experimental methods

The cross-section measurements have been carried out at LUNA2 electrostatic continuous beam 400 kV accelerator that provides an ${}^4\text{He}^+$ beam of 0.3 mA average intensity. Since the cross-section is of the order of nanobarn, the expected counting rate is very low indeed, therefore special attention must be paid to any possible sources of background in the experimental setup. LUNA can exploit 1400 m of rock as a powerful passive shield from cosmic ray, with a measured reduction of 10^6 of the muon flux with respect to the surface. Figure 1 shows the experimental setup (see Anders et al. (2013) for more details). The nuclear reactions are induced in a windowless differentially pumped gas target filled with up to 0.3 mbar (0.25% precision) high purity (99.8% chemical and isotopic purity) deuterium gas. The emerging γ -rays have been detected by a large (137% relative efficiency) high-purity germanium (HpGe) spectrometer placed at 90° with respect to the incident ${}^4\text{He}^+$ beam, in very close geometry to optimize the detection solid angle. The natural background of LNGS is further reduced up to three orders of magnitude in

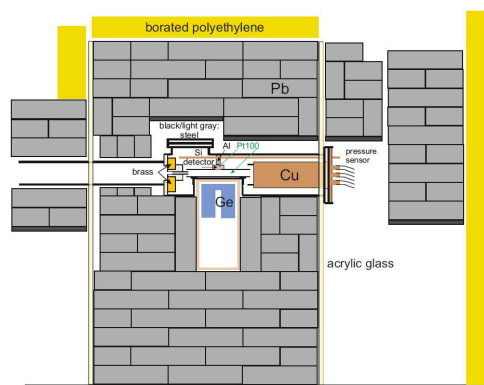


Fig. 1. The chamber of the windowless gas target is seen near the center. The inner lead castle is surrounded by an anti-radon box made of acrylic glass.

the γ -ray continuum below 2615 keV (Cacioli et al. 2009) by means of a 4π lead shield around the reaction chamber and the HpGe detector. An extra shield of high density polyethylene (5% boron enriched) is mounted around the gas target.

The main source of the physics background is of beam-induced nature and is mainly due to neutron interactions on structural and shielding material, especially on the germanium detector itself. Unfortunately these neutrons give rise to a large Compton background in the ${}^2\text{H}(\alpha, \gamma){}^6\text{Li}$ region of interest. For this reason, at the centre of the target chamber, a smaller box-shaped AISI 304 steel inner tube of $1.8 \times 1.8 \text{ cm}^2$ area and 17 cm length with a wall thickness of 1 mm was introduced. This inner tube limits the lateral length that the scattered deuterons travel inside the gas.

4. Discussion

If one assumes that the ${}^2\text{H}(\alpha, \gamma){}^6\text{Li}$ cross section is equal to the recommended value from Robertson et al. (1981), at $E_\alpha = 400 \text{ keV}$ a signal-to-noise ratio of about 1:12 is obtained with the present neutron induced background. Therefore, it is important that the background level is understood with a precision on the percent level, we think the present analysis has reached such a precision, for the analy-

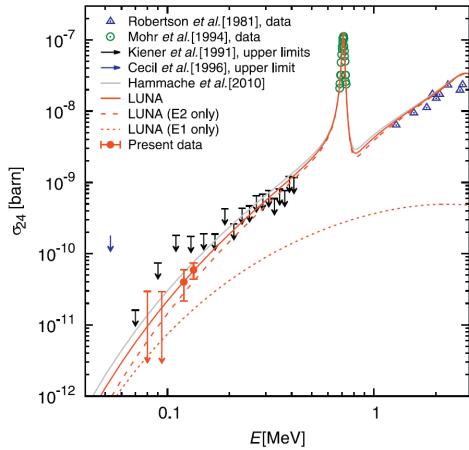


Fig. 2. Cross section of the ${}^2\text{H}(\alpha, \gamma){}^6\text{Li}$ reaction. The LUNA data and our recommended curves are reported in red.

sis details see Anders et al. (2013). In order to compute the thermonuclear reaction rate for the temperatures of interest in BBN, in addition to the present cross-section data, some assumptions have to be made on the behavior of the cross section at different energies. The total cross section is given by the sum of electric dipole ($E1$) and quadrupole ($E2$) contributions. The $E2$ contribution is relatively well-constrained by the direct measurement around the $E_\alpha = 0.711$ MeV resonance. Therefore, for the reaction rate determination, the $E2$ contribution given by the theoretical work of Mohr et al. (1994) is adopted here. The situation is different for the $E1$ contribution which is only constrained by the LUNA data. In order to tackle this problem, the Hammache et al. (2010) $E1$ curve is rescaled so that the sum of $E1$ and $E2$ curves match the present data. As the $E1$ component gives only a very small contribution at high energy, this scaling does not affect the good match of theoretical $E2$ curve and previous high-energy data (see Fig. 2). The thermonuclear reaction rate obtained based on our data is much lower than the previous rate by Caughlan & Fowler (1988), but also lower than all other previously reported thermonuclear reaction rates (Hammache et al. 2010; Mukhamedzhanov et al. 2011; Angulo

et al. 1999) (see Fig. 2). The relative uncertainty of the present rate is 25%, given by the systematic and statistical errors of the present data, combined in quadrature. The impact of the present new thermonuclear reaction rate on the amount of ${}^6\text{Li}$ produced in BBN was investigated. A BBN calculation has been performed with the code described in (Smith et al. 1993). In the computation, values for the neutron lifetime of 880.1 s and for the final baryon-to-photon ratio of $\eta = 6.102 \times 10^{-10}$ have been used. The nuclear reaction rates were kept unchanged, except for the presently updated ${}^2\text{H}(\alpha, \gamma){}^6\text{Li}$ rate. The resulting abundance is ${}^6\text{Li}/\text{H} = (0.80 \pm 0.18) \times 10^{-14}$, 27% lower than the value obtained when using the rate in Caughlan & Fowler (1988) for ${}^2\text{H}(\alpha, \gamma){}^6\text{Li}$. As a further step, also the ${}^6\text{Li}/{}^7\text{Li}$ isotopic ratio from BBN has been determined, in order to enable a comparison with the observations in metal poor stars that usually report ${}^6\text{Li}/{}^7\text{Li}$ isotopic ratios. For this purpose, ${}^3\text{He}(\alpha, \gamma){}^7\text{Be}$ reaction rate evaluated in Kontos et al. (2013) is used, which is within 1.5% of the value presented in deBoer et al. (2014) and Takács et al. (2015) rates. The excitation function adopted in that work closely tracks the LUNA data on ${}^3\text{He}(\alpha, \gamma){}^7\text{Be}$ (Bemmerer et al. 2006; Confortola et al. 2007), which are direct experimental data on this reaction at energies below 300 keV, most relevant for BBN. Therefore, by using the rate in (Kontos et al. 2013) the ${}^6\text{Li}/{}^7\text{Li}$ isotopic ratio is determined by the ratio of two LUNA experimental S-factors in similar setups: the present ${}^2\text{H}(\alpha, \gamma){}^6\text{Li}$ data on ${}^6\text{Li}$ production, and the previous ${}^3\text{He}(\alpha, \gamma){}^7\text{Be}$ data (Bemmerer et al. 2006; Confortola et al. 2007) on ${}^7\text{Be} \rightarrow {}^7\text{Li}$ production. Figure 3 shows the LUNA astrophysical S factor for ${}^2\text{H}(\alpha, \gamma){}^6\text{Li}$ compared with literature data and theoretical curves, in good agreement with Tursunov et al. (2018). Using the rate of (Kontos et al. 2013), ${}^7\text{Li}/\text{H} = (5.2 \pm 0.4) \times 10^{-10}$ is found, 15% higher than when using Caughlan & Fowler (1988). Finally, a lithium isotopic ratio of ${}^6\text{Li}/{}^7\text{Li} = (1.5 \pm 0.3) \times 10^{-5}$ is obtained, lower than the value of 2.3×10^{-5} of (Coc et al. 2012), that did not make use of the present data. The ${}^6\text{Li}/{}^7\text{Li}$ error is dominated by the 22% uncertainty on ${}^6\text{Li}$ while the ${}^7\text{Li}$ abundance pre-

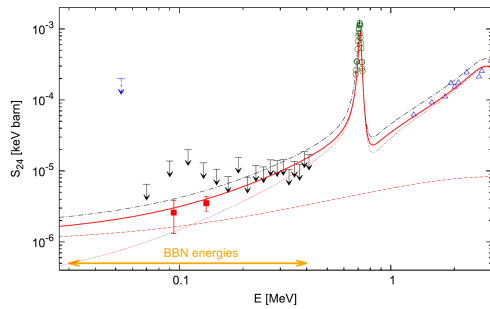


Fig. 3. Astrophysical S factor of ${}^2\text{H}(\alpha, \gamma){}^6\text{Li}$ reaction from LUNA (red squares, Anders et al. 2014) and literature: blue triangles (Robertson et al. 1981); green circles (Mohr et al. 1994); black arrows (Kiener et al. 1991); blue dashed arrow (Cecil et al. 1996); red long dashed E1, red short dashed E2 and red full E1+E2 (Mukhamedzhanov et al. 2011); black dot dashed E1+E2 (Hammache et al. 2010).

diction is known at the 8% (Coc et al. 2014). These ${}^6\text{Li}/{}^7\text{Li}$ ratios are much lower than the ones obtained from the ${}^6\text{Li}$ astronomical measurements in metal-poor stars (Asplund & Meléndez 2008; Steffen et al. 2012) and in the Small Magellanic Cloud (Howk et al. 2012). Further astronomical investigations and astrophysical modelling are desirable. Assuming that future observations will confirm a somewhat higher ${}^6\text{Li}$ abundance with respect to the computed ΛCDM (Lambda Cold Dark Matter) model, the only remaining possibilities to explain the discrepancy are very special astrophysical processes like stellar flare in-situ lithium production (Prantzos 2012) and/or new physics scenarios (Pospelov & Pradler 2010; Trezzi et al. 2017).

References

- Anders, M., Trezzi, D., Bellini, A., et al. 2013, *European Physical Journal A*, 49, 28
- Anders, M., Trezzi, D., Menegazzo, R., et al. 2014, *Phys. Rev. Lett.*, 113, 042501
- Angulo, C., Arnould, M., Rayet, M., et al. 1999, *Nuclear Physics A*, 656, 3
- Asplund, M., et al. 2006, *ApJ*, 644, 229
- Asplund, M. & Meléndez, J. 2008, in *First Stars III*, American Institute of Physics, ed. B. W. O’Shea, A. Heger & T. Abel (AIP, Melville, NY), AIP Conf. Proc., 990, 342
- Baur, G. & Rebel, H. 1996, *Annual Review of Nuclear and Particle Science*, 46, 321
- Bemmerer, D., Confortola, F., Costantini, H., et al. 2006, *Phys. Rev. Lett.*, 97, 122502
- Caciolli, A., Agostino, L., Bemmerer, D., et al. 2009, *The European Physical Journal A*, 39, 179
- Caughlan, G. R. & Fowler, W. A. 1988, *Atomic Data and Nuclear Data Tables*, 40, 283
- Cecil, F., Yan, J., & Galovich, C. S. 1996, *Physical Review C*, 53, 1967
- Coc, A., et al. 2012, *ApJ*, 744, 158
- Coc, A., Uzan, J.-P., & Vangioni, E. 2014, *Journal of Cosmology and Astroparticle Physics*, 2014, 050
- Confortola, F., Bemmerer, D., Costantini, H., et al. 2007, *Phys. Rev. C*, 75, 065803
- deBoer, R. J., Görres, J., Smith, K., et al. 2014, *Phys. Rev. C*, 90, 035804
- Fields, B. D. 2011, *Annual Review of Nuclear and Particle Science*, 61, 47
- Hammache, F., Heil, M., Typel, S., et al. 2010, *Physical Review C*, 82, 065803
- Hinshaw, G., Larson, D., Komatsu, E., et al. 2013, *ApJS*, 208, 19
- Howk, J. C., Lehner, N., Fields, B. D., & Mathews, G. J. 2012, *Nature*, 489, 121
- Kiener, J., Gils, H., Rebel, H., et al. 1991, *Physical Review C*, 44, 2195
- Kontos, A., Uberseder, E., deBoer, R., et al. 2013, *Phys. Rev. C*, 87, 065804
- Korn, A. J., Grundahl, F., Richard, O., et al. 2006, *Nature*, 442, 657
- Lind, K., et al. 2013, *A&A*, 554, A96
- Mohr, P., Kölle, V., Wilmes, S., et al. 1994, *Physical Review C*, 50, 1543
- Mukhamedzhanov, A., Blokhintsev, L., & Irgaziev, B. 2011, *Physical Review C*, 83, 055805
- Nollett, K. M. 2001, *Physical Review C*, 63, 054002
- Pérez, A. G., Aoki, W., Inoue, S., et al. 2009, *A&A*, 504, 213
- Pospelov, M. & Pradler, J. 2010, *Annual Review of Nuclear and Particle Science*, 60, 539
- Prantzos, N. 2012, *A&A*, 542, A67
- Reeves, H., Fowler, W., & Hoyle, F. 1970, *Nature*, 226, 727

- Robertson, R., Dyer, P., Warner, R., et al. 1981, *Physical Review Letters*, 47, 1867
- Serpico, P. D., Esposito, S., Iocco, F., et al. 2004, *Journal of Cosmology and Astroparticle Physics*, 2004, 010
- Smith, M. S., Kawano, L. H., & Malaney, R. A. 1993, *ApJS*, 85, 219
- Spite, M. & Spite, F. 1982, *Nature*, 297, 483
- Steffen, M., et al. 2010, *IAU Symposium*, 268, 215
- Steffen, M., Cayrel, R., Caffau, E., et al. 2012, *Memorie della Società Astronomica Italiana Supplementi*, 22, 152
- Takács, M. P., et al. 2015, *Phys. Rev. D*, 91, 123526
- Trezzi, D., Anders, M., Aliotta, M., et al. 2017, *Astroparticle Physics*, 89, 57
- Tursunov, E. M., et al. 2018, *Phys. Rev. C*, 98, 055803